In-vivo classification of trabecular bone rods and plates via local inertial anisotropy (LIA)

B. Vasilic[1], J. F. Magland[1], and F. W. Wehrli[1]

[1]Laboratory for Structural NMR Imaging, Department of Radiology, University of Pennsylvania School of Medicine, Philadelphia, PA, United States

INTRODUCTION

Trabecular bone (TB), an intricate network of bony rods and plates, is found in long bones, the vertebrae and other skeletal sites. Most fractures occur at sites rich in trabecular bone, with about 60% of bone's strength attributed to its mineral density. Recent research indicates that the remaining 40% variation in bone strength can be explained by its micro-structure. Trabecular plates are oriented parallel to the local loading direction with rods supporting the plates against buckling in the perpendicular direction. A key parameter describing TB micro-architecture is the ratio of plate-like to rod-like structures, reflecting the mechanical strength of the architecture. Recent advances [1] in high-resolution MRI have allowed in-vivo imaging of the trabecular network with sufficient resolution and image quality for quantitative analysis and structural classification [2]. Analysis of MR images of TB is challenging because of the fairly low signal to noise ratio (SNR) of the images (~10) and partial volume effects resulting from the very small scale of the imaged structures (~100μm). Here we introduce a new, gray-scale based method that classifies TB structures into rods and plates and determines their orientation using an analogy to rigid body mechanics.

THEORY

Let us denote the image intensity at voxel r with $m(r)$. In the case of an MR image of TB this intensity is proportional to the bone marrow density weighted by the coil sensitivity profile. If we invert the intensity values by subtracting them from their maximum value the resulting image, $b(r)$, will reflect the local bone density. We define the local tensor of inertia, $I(r)$, at voxel r of the density $b(r)$ as

$$I(r)=\sum b(r+r')[r'^{2}-|r'><r'|], \qquad (1)$$

where the vector r' takes values within a ball of radius s centered at r and the second term in the sum is the diad formed by that vector. $I(r)$ will reflect the mechanical properties of the bone density, and its eigenvalues, $\lambda_1 < \lambda_2 < \lambda_3$, can be used to classify structures into rods and plates. We define $c=2(\lambda_2-\lambda_1)/(\lambda_3-\lambda_1)-1$, a classification parameter that takes values from -1 to 1. For oblate, plate-like structures the two smallest eigenvalues, λ_1 and λ_2, will be closer together than the two largest eigenvalues, λ_2 and λ_3, leading to a negative value of c. The eigenvector corresponding to the largest eigenvalue, λ_3, will be perpendicular to the oblate plane of the structure determining the orientation of the plate. Rod-like structures have the two largest eigenvalues closer together, $c>0$, with the eigenvector corresponding to λ_1 determining the orientation of the rod, as illustrated in Fig. 1. Structures for which $c=0$ are neither plates nor rods and are found in regions joining plate-like and rod-like structures (Fig. 2). The sign of c thus determines whether a structure is plate or rod-like, while its absolute value measures how plate-like or rod-like the structure is.

Local inertial anisotropy (LIA), as described above, produces a continuous classification of voxels as belonging to rod-like or plate-like structures and can be applied to both gray-scale and segmented images. Scaling the image intensity scales the eigenvalues of $I(r)$ (see Eq. 1) and does not change the classification (i.e. ratios of eigenvalues), or the corresponding orientation of the structures. Since $I(r)$ is calculated over a ball neighborhood, a constant offset in the image intensity produces an isotropic (scalar) correction to $I(r)$ which also does not affect the classification. LIA is also robust to noise corruption since spatially homogeneous noise produces an approximately isotropic tensor of inertia within the ball neighborhood. The variations in $I(r)$ introduced by noise are not biased since the $I(r)$ is linear in the image intensity. Thus, the *mean values* of the noise corrupted classification should not depend on the amount of noise present in the image.

METHODS

The algorithm was implemented in C++ and integrated into a graphical user interface (GUI) based on the Qt framework (Trolltech ASA). The GUI allowed for single image and batch processing as well as interactive visualization of both classification and orientation (Fig. 2). Two variants of the algorithm were implemented. LIA applied to gray-scale inputs, followed the description above. For binary (segmented into object and background) datasets the analysis was applied only to points belonging to the object region. The $I(r)$ was calculated not in the ball neighborhood of each object point but for a connected region of linear dimensions s resulting from a region-growing procedure with the initial point as the seed. This modified algorithm removed edge effects in segmented data and produced classifications in excellent agreement with the heuristically expected results as shown in Fig. 2. The plate to rod ratio $\eta=(\sum_{c(r)<0} b(r)|c(r)|)/(\sum_{c(r)>0} b(r)|c(r)|)$ was used to quantify the calculated classification.

RESULTS

The method was validated on 8 binarized micro-CT images of the human radius acquired at $(16\mu m)^3$ voxel size. Each image was down-sampled to progressively lower resolutions - $(32\mu m)^3$, $(64\mu m)^3$, $(128\mu m)^3$ - using appropriately reduced regions of k-space from the Fourier transform of the original image. As Fig. 3a) illustrates differences in η are preserved between most specimens down to the lowest resolution. The sensitivity of the method to SNR variations was explored by corrupting the lowest resolution, $(128\mu m)^3$ voxel size, images with varying levels of noise. Fig. 3b) shows that, while there is a change in η as SNR decreases, this change is systematic and preserves the differences in η between specimens. The largest change in η from its value at SNR=4 to its value at SNR=25 is ~40% and for most specimens the change from SNR=8 to SNR=25 is less than 20%. LIA analysis was also applied to two in-vivo MR datasets acquired in an ongoing clinical study of testosterone deficient men. The images were processed using the Virtual Bone Biopsy [1] and their skeletons classified using the second variant of LIA, intended for binary data. Fig. 4 illustrates the difference in architecture between the two images, with one (left) having a plate-to-rod ratio of 2.9 and the other (right) a plate-to-rod ratio of 2.3. Further evaluation of LIA is currently under way on in-vivo MR data.

[1] F. W. Wehrli, P. K. Saha, B. R. Gomberg and H. K. Song, Proceedings of the IEEE 91 (10): 1520-1542 (2003).
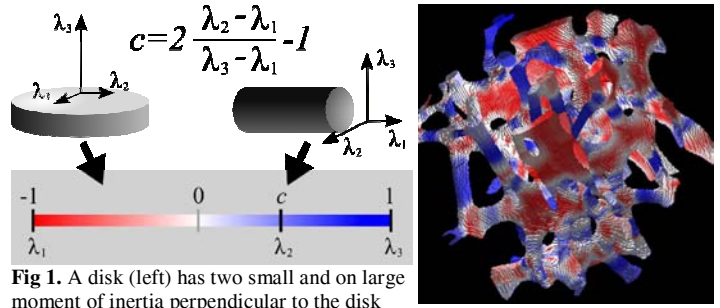[2] P. K. Saha and F. W. Wehrli, Pattern Recognition 37 (9): 1935-1944 (2004).

$$c=2\frac{\lambda_2-\lambda_1}{\lambda_3-\lambda_1}-1$$

Fig 1. A disk (left) has two small and on large moment of inertia perpendicular to the disk plane. A cylinder (right) has two large and one small moment of inertia parallel to its axis. Color scale (bottom) assigning red to plates and blue to rods.
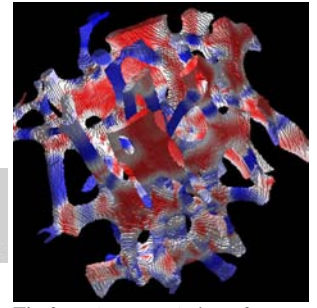

Fig 2. Volume rendering of a micro-CT scan from the human radius with voxels color coded according to classification.
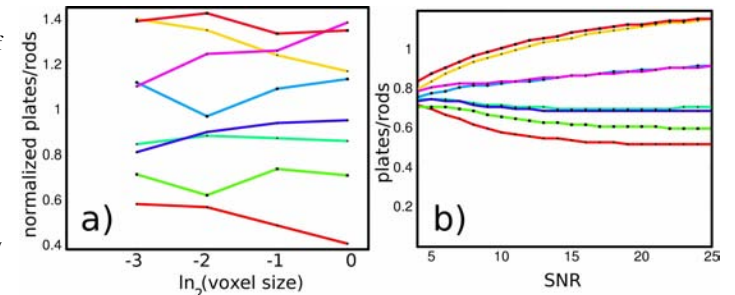

Fig. 3. a) Plate-to-rod ratio as a function of the $\log_2$ of the voxel size divided by the micro-CT resolution (16μm). The plate-to-rod ratio was normalized to its mean value (over all specimens) at a given resolution to emphasize changes. b) Plate-to-rod ratio as a function of SNR for the lowest resolution images.
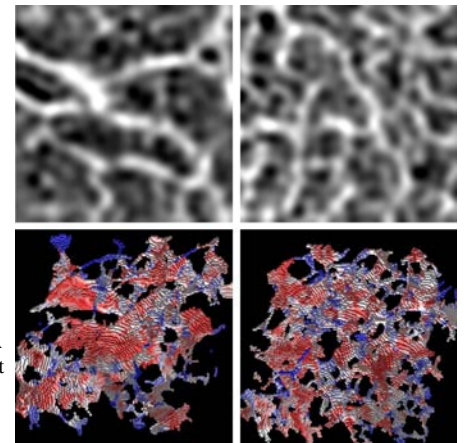

Fig. 4. Top row: Volumes of interest of MR images acquired and processed with the Virtual Bone Biopsy. Bottom row: LIA classified skeletons of the above images.